INTERNATIONAL JOURNAL FOR NUMERICAL AND ANALYTICAL METHODS IN GEOMECHANICS
Int. J. Numer. Anal. Meth. Geomech., **22**, 819–850 (1998)

STOCHASTIC FINITE ELEMENT METHODS FOR THE SEISMIC RESPONSE OF SOILS

C. H. YEH AND M. S. RAHMAN*

Department of Civil Engineering, Box 7908, North Carolina State University, Raleigh, NC 2795-7908, U.S.A.

SUMMARY

Some of the available stochastic finite element methods are adapted and evaluated for the analyses of response of soils with uncertain properties subjected to earthquake induced random ground motion. In this study, the dynamic response of a soil mass, with finite element discretization, is formulated in the frequency domain. The spectral density function of the response variables are obtained from which the evaluation of the root-mean-squared and the most probable extreme values of the response are made. The material non-linearities are incorporated by using strain compatible moduli and damping of soils using an equivalent linear model for stress–strain behaviour of soils and an iterative solution of the response. The spatial variability of the shear modulus is described through a random field model and the earthquake included motion is treated as a stochastic process. The available formulations of direct Monte-Carlo simulation, first-order perturbation method, a spectral decomposition method with Neumann expansion and a spectral decomposition method with Polynomial Chaos are used to develop stochastic finite element analyses of the seismic response of soils. The numerical results from these approaches are compared with respect to their accuracy and computational efficiency. © 1998 John Wiley & Sons, Ltd.

Key words: stochastic; finite element; seismic; response; random; variability

1. INTRODUCTION

The evaluation of seismic responses of soils constitutes an important problem in relation to the ground motion amplification and the instability of soils. The ground motion generated by an earthquake is a random process. Details of input motions have significant effects on the response of soils masses which has been demonstrated by the wide range of variability in the response reported by different researchers.[1,2] Also, there always exist uncertainties in defining the properties of soils. This results from: (i) natural heterogeneity or the variability of the soil, (ii) limited availability of information and (iii) measurement errors. These uncertainties associated with system parameters are also likely to have an influence on the response,[3,4]

The recent development of the stochastic finite element methods provides a rational framework for the analysis of complex uncertain systems subjected to stochastic excitation. The terminology 'stochastic finite element method' is frequently used to denote the application of finite element methods for the analysis of systems with parametric uncertainties, whether or not the inputs are

* Correspondence to: M. S. Rahman, Department of Civil Engineering, Box 7908, North Carolina State University, Raliegh, NC 27695-7908, U.S.A. E-mail: rahman@eos.ncsu.edu.

CCC 0363–9061/98/100819–32$17.50

Received 25 July 1997
Revised 24 November 1997

random. Many researchers have contributed to the earlier development of the field. Applications of the stochastic finite element analysis have also been made to some geotechnical problems.[5,6]

The response of a discrete system with uncertain parameters, when dynamic loads are considered, is commonly determined by using simulation techniques[7,8] or perturbation methods.[9,10] Perturbation and simulation-based stochastic finite element methods have been applied to study the seismic response variability of soil sites.[11,12] Simulation methods are quite powerful, but in general, in addition to being computationally very extensive, they provide limited insight into the behaviour and sensitivity of the system. In perturbation methods, uncertainties have to be small and they usually have problems with accuracy and convergence. In recent years, other methods of evaluating the response of uncertain systems have been proposed. Igusa and Der Kiureghian[4] used the framework of first and second-order reliability methods to investigate the variability of dynamic response of uncertain systems to stochastic excitation. Spanos and Ghanem[13] make use of the Karhunen–Loeve expansion to represent the random material property. The expansion is a representation of the process in terms of a finite set of uncorrelated random variables. A Neumann expansion scheme is subsequently used to obtain a convergent expansion of the response process. Later Ghanem and Spanos[14] used spectral expansion in terms of polynomial chaos instead of Neumann expansion. Along a similar line, Jensen and Iwan[15,16] have developed an alternative method to evaluate the dynamic response of a discrete uncertain system subjected to stochastic excitation based on the expansion of the response in terms of a series of polynomials that are orthogonal.

In this study, the general framework of some available formulations are used to develop stochastic finite element methods for the analysis of the seismic response of soils. The seismically induced ground acceleration is treated as a random process. A finite element formulation is used to discretize the soil mass and its dynamic response is formulated in the frequency domain with transfer functions for various parameters, viz., displacement, acceleration, strain and stress. The spectral density functions of these response variables are then obtained, from which the calculations for the root mean squared and their most extreme values are made. The material non-linearities are incorporated by using strain compatible moduli and damping of soils using the equivalent linear model for stress–strain behaviour of soils and interative solution of the response.

The spatial variability of the shear modulus is described through a random field model which is also discretized through the finite element mesh. Thus, the random input (for shear modulus) consists of a vector of random variables (i.e. the local average across each element) whose covariance matrix depends on the finite element mesh. Four stochastic finite element methods, direct Monte Carlo simulation, first-order perturbation method, a spectral decomposition method with Neumann expansion, and a spectral decomposition method with polynomial chaos are adapted and evaluated for the analysis of the seismic response of soils. Few illustrative numerical results from these methods are presented and compared to evaluate their accuracy and computational efficiency. The focus in this paper is on different methodologies of stochastic finite element analysis and an evaluation of their usage for the analysis of seismic response of soils. For convenience of presentation, all the formulations presented here are for one-dimensional systems only. An extension to two-dimensional system representing earth structures can readily be made.

2. RANDOM GROUND MOTION

In this study, for simplicity and ease of analysis, the ground motion is considered to be a stationary random process (with constant frequency content) truncated for a finite duration.

The following power spectral density function suggested by Kanai and Tajimi is used to characterize a strong earthquake ground motion

$$S_{\ddot{u}_g} = \frac{S_0\,(1 + 4\zeta_g^2\,(\omega/\omega_g)^2)}{[1 - (\omega/\omega_g)^2]^2 + 4\zeta_g^2\,(\omega/\omega_g)^2} \tag{1}$$

In the above, ω is component frequency, S_0 is the scale factor, ω_g and ζ_g are the equivalent natural frequency and damping ratio of the ground characterized by a single-degree-of-freedom system. Two statistical parameters of the given spectral density function are of special interest, which are defined in terms of the following spectral moments,

$$\lambda_i = \int \omega^i\, S_{\ddot{u}_g}(\omega)\, \mathrm{d}\omega, \quad i = 0, 1, 2, \ldots \tag{2}$$

The RMS of the ground acceleration $\sigma_{\ddot{u}_g}$ and the central frequency Ω are given as

$$\sigma_{\ddot{u}_g} = \sqrt{\lambda_0} \tag{3}$$

$$\Omega = \sqrt{\lambda_2/\lambda_1} \tag{4}$$

The ground motion, thus characterized, represents a stationary random motion obtained by filtering a white noise. In order to approximate the non-stationarity of the actual ground motion, only a segment of the stationary motion, defined as equivalent stationary duration is used. A simple procedure proposed by Hou[17] is followed for this purpose. A tree segment envelope (Figure 1), consisting of a segment of buildup followed by a segment of constant intensity and a segment of decay, is used to define the intensify function:

$$I(t) = E\,[\ddot{u}_{g\max}]\;\Delta_{\ddot{u}_g}\,F_0\psi_0 \tag{5}$$

$E\,[\ddot{u}_{g\max}]$ is the expected maximum acceleration, which can be calculated from the earthquake magnitude, M_e, and the epicentral distance, R (in (km), by the following relation[18]

$$E\,[\ddot{u}_{g\max}] = 1230\,e_{0\cdot 8M}\,(R + 25)^{-2} \tag{6}$$

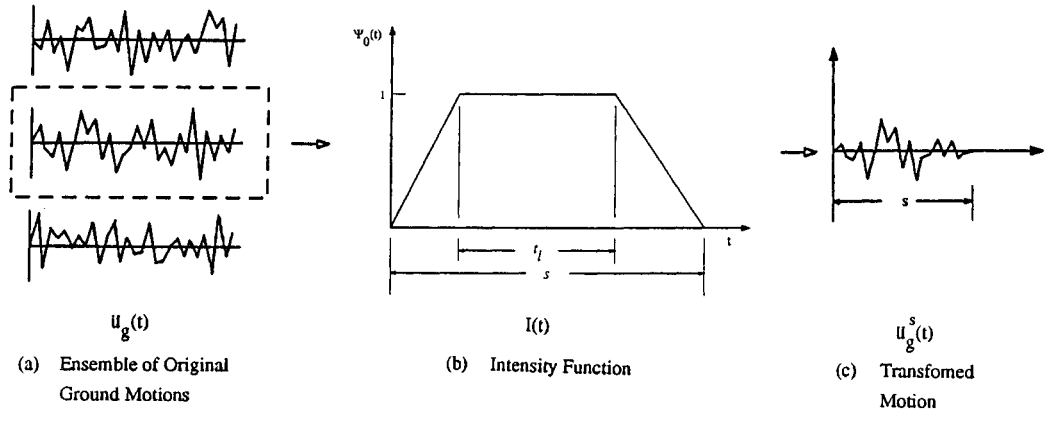

Figure 1. Random ground motion

Here, acceleration is expressed in cm/s^2. The correlation factor, $\Delta_{\ddot{u}_g} = 2{\cdot}05$, is used to account for the uncertainty associated with the above results, which is the mean ratio between the observed and the calculated value of $E[\ddot{u}_{g\max}]$. The non-stationary behaviour of the motion if accounted for by the shape function $\psi_0 = \psi_0(t)$, illustrated in Figure 1. For peak value statistics, the non-stationary process will be replaced by an equivalent stationary motion with a duration $T(= c_0 s)$ shorter than the actual duration s of the earthquake. The scaling factor, F_0, is defined as the ratio of the standard deviation of acceleration amplitude, $\sigma_{\ddot{u}_g}$, to the expected highest peak of the process, during a finite duration s. According to Hou, F_0 is given as

$$F_0 = \frac{\sigma_{\ddot{u}_g}}{E[\ddot{u}_{g\max}]\ \Delta\ddot{u}_g} = [2\ln((2c_0 s)/T_a)]^{-0{\cdot}5} \tag{7}$$

where

$$c_o = 0{\cdot}25 + 0{\cdot}75\, t_l/s \tag{8}$$

In the above, T_a is the expected mean period of the excitation, which is suggested to be 0·2246 s ($\omega_a = 8{\cdot}9044\,\pi$). The t_l defined in Figure 1 is the strong motion duration.

From the above equations and noting that $\psi_0(t) = 1$ for the strong portion of the record, one can obtained the variance of the excitation process in the form of

$$\sigma^2_{\ddot{u}_g} = \frac{E^2[\ddot{u}_{g\max}]\,\Delta^2_{\ddot{u}_g}}{2\ln\ (2c_0\ s/T_a)} \tag{9}$$

which is suitable for peak statistical calculations. The scale factor S_0 can then be calculated, based on equation (3), as

$$S_0 = \frac{4\zeta_g\,\sigma^2_{\ddot{u}_g}}{\omega_g\ (1 + 4\zeta_g^2)} \tag{10}$$

The natural frequency of the ground motion is in the range of $2{\cdot}1 < \omega_g < 21$, and the damping ratio $\zeta_g = 0{\cdot}64$. The mean and standard deviation of ω_g and ζ_g for different site conditions are available.[19] By using S_0, ω_g and ζ_g, in equation (1), the spectral density found can be obtained

3. RANDOM FIELD MODEL FOR SOIL PROPERTIES

In order to describe the variability of soil properties a random field model[20,21] is used. In this approach a homogeneous random field $u(z)$ is characterized (Figure 2) by these parameters: (1) the average value $\bar{u}$, (ii) the standard deviation or root-mean-square (rms) fluctuation of $u(zx)$, which measures the intensity of fluctuation or degree to which actual value of $u(z)$ may deviate from $\bar{u}$ and (iii) the scale of fluctuation, δ_u, which measures the distance within which the soil property $u(z)$, shows relatively strong correlation or persistence from point to point. Small values of δ_u imply rapid fluctuation about the average, while large values δ_u suggest that a slowly varying component is superimposed on the average value of u.

The variation of soil property $u(z)$ can be represented by constant mean trend $\bar{u}(z)$ and a zero-mean random field $\alpha(z)$ as

$$u(z) = \bar{u}(z) + \alpha(z) \tag{11}$$

Using the first and second-order statistical moments the variation of $u(z)$ is described by

$$E[u(z)] = \bar{u}(z) \tag{12}$$

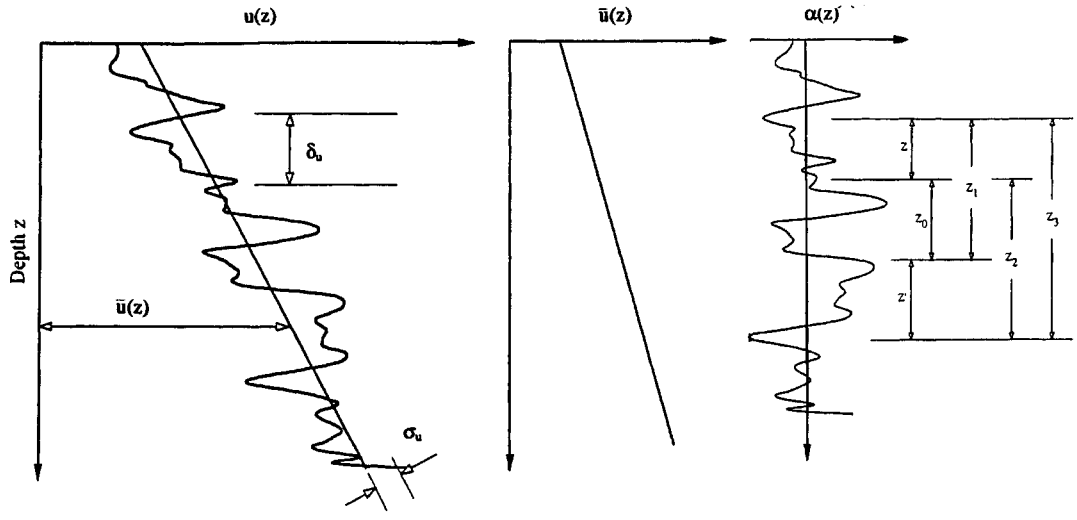

Figure 2. Variability of soil properties: random field model

$$\mathrm{Var}[u(z)] = \mathrm{Var}[\alpha(z)] = \sigma_\alpha^2 = \text{constant} \tag{13}$$

$$\mathrm{Cov}(u(z),\, u(z+\xi)] = R_{\alpha\alpha}(\xi) = \sigma_\alpha^2\, \rho_\alpha(\xi) \tag{14}$$

In the above $E[\cdot]$, $\mathrm{Var}[\cdot]$ and $\mathrm{Cov}[\cdot]$ are the expected value, variance and covariance, respectively; $\rho_\alpha(\xi)$ is the coefficient of correlation of α. For very small interval ξ, the coefficient of correlation will be close to 1 but will decay as the interval increases. Many specific analytical expressions have been proposed[20] for the autocorrelation function, $R_{\alpha\alpha}(\xi)$.

In the stochastic finite element analysis, an average soil property is assumed over an element. A one-dimensional random field $u(z)$ with mean $\bar{u}(z)$ and variance σ_α, its local averages process $u_Z(z)$ of $u(z)$ over the interval Z centred at z (Figure 2) is defined as

$$u_Z(z) = \frac{1}{Z}\int_{z-Z/2}^{z+Z/2} u(z')\,\mathrm{d}z' \tag{15}$$

The above local average will vary depending upon the specific location of the interval Z within the 'statistically homogeneous' soil layer. Simplifying the notation $u_Z(z)$ as u_Z, mean and variance of this average process are given by

$$\begin{aligned} E[u_Z] &= E[u(z)] = \bar{u}(z) \\ \mathrm{Var}[u_Z] &= \mathrm{Var}[\alpha_Z] = \sigma_\alpha^2\, \gamma(Z) \end{aligned} \tag{16}$$

where $\gamma(Z)$ is the variance reduction function of $\alpha(z)$, which measures the reduction of the point variance σ_α^2 under local average. Vanmarcke[20] suggested the variance function as

$$\begin{aligned} \gamma(Z) &= 1 \quad \text{for } Z \leqslant \delta \\ \gamma(Z) &= \frac{\delta}{Z} \quad \text{for } Z \geqslant \delta \end{aligned} \tag{17}$$

The covariance of α_{Z_1} and α_{Z_2}, of the process $\alpha(z)$, corresponding to two segments Δz_1 and Δz_2 (Figure 2) is expressed as

$$\text{Cov}\,[\alpha_{Z_1}, \alpha_{Z_2}] = \sigma_\alpha^2\, B\,(Z_1, Z_2) \tag{18}$$

where

$$B(Z_1, Z_2) = \frac{Z_0^2\,\gamma\,(Z_0) - Z_{01}^2\,\gamma\,(Z_{01}) - Z_{02}^2\,\gamma(Z_{02}) + Z_{012}^2\,\gamma\;(Z_{012})}{2Z_1Z_2} \tag{19}$$

in which, $Z_1 = \Delta z_1,\ Z_2 = \Delta z_2,\ Z_0 = \Delta z_0,\ Z_{01} = \Delta z_1 + \Delta z_0,\ Z_{02} = \Delta z_2 + \Delta z_0$ and $Z_{012} = \Delta z_1 + \Delta z_0 + \Delta z_2$. From the above equations, the matrix ,of covariance of pairs of spatial average of the random field $u(z)$ can be calculated.

4. STOCHASTIC FINITE ELEMENT METHODS

4.1. Preliminaries

The elements common to all the stochastic finite element analyses used in the study are outlined first. Subsequently, the formulations of different Stochastic Finite Element Methods (SFEM) are presented separately.

4.1.1. Seismic responses of soils. The seismic response of a horizontally layered soil site is assumed to be caused primarily by the vertical propagation of shear waves from the underlying formation. Considering the soil to be a linear Coulomb-damped elastic system, the responses is assumed to be goverened by the following wave equation:

$$\rho\,\frac{\partial^2 u}{\partial t^2} = G^*\,\frac{\partial^2 u}{\partial z^2} \tag{20}$$

with $G^* = G\,(1 + 2\mathrm{i}\beta)$.

In the above, u is horizontal displacement, ρ is the density of soil mass, G^* is the complex shear modulus, G is the shear modulus and β is the damping ratio resulting from the frictional loss of energy. Here, G and β and hence G^* are assumed to be independent of frequency in accordance with the experimentally observed behaviour of soils.

In this study, the shear modulus is assumed to constitute a random field. It can be decomposed into a trend component $\bar{G}$ and random component α_G, that is

$$G(z) = \bar{G}(z) + \alpha_G(z) \tag{21}$$

in which $\bar{G}(z)$ is the mean value of shear modulus at z, and $\alpha_G(z)$ is a zero mean, multidimensional and uni-variate real homogeneous random field with the autocorrelation function $R_{\alpha\alpha}(z_1, z_2)$ associated with location z_1 and z_2. The autocorrelation function is assumed to be of the following form:

$$R_{\alpha\alpha}(z_1, z_2) = \sigma_G^2\ \mathrm{e}^{-|z_1 - z_2|/b} \tag{22}$$

in which σ_G denotes the standard deviation of the random process under consideration. While b is a parameter called correlation length which equals one-half of the scale of the fluctuation defined in the previous section.

4.1.2. Finite element formulation. For a soil site discretized with a system of element Ω^e subjected to horizontal ground excitation, $\ddot{u}_g$, the equation of motion can be written as

$$M\ddot{u} + Ku = -m\ddot{u}_g \tag{23}$$

where $\ddot{u}$ and u are acceleration and displacement vectors, respectively. In the right-hand side $m(=M\delta)$ is the mass vector in which δ is the influence factor, and $\delta_i = 1$, if the degree of freedom is the same as the direction of ground motion; otherwise $\delta_i = 0$. The global mass matrix, M, and stiffness matrix K, are obtained by assembling the element mass and stiffness matrices over the entire region as

$$M = \sum_{e=1}^{N} M_e, \qquad K = \sum_{e=1}^{N} K_e \tag{24}$$

in which N is the total number of elements and the summation implies the addition of the appropriate location to the matrix. The element stiffness matrix is

$$K_e = \frac{G_e^*}{l_e}\begin{bmatrix} 1 & -1 \\ -1 & 1 \end{bmatrix} \tag{25}$$

While the consistent mass matrix of element e can be obtained as

$$M_e = \frac{\rho_e l_e}{6}\begin{bmatrix} 2 & 1 \\ 1 & 2 \end{bmatrix} \tag{26}$$

In the above, G_e^* and ρ_e are the spatial average of the modulus and density of the soil in the element e with a length l_e.

4.1.3. Response function. To solve the equation (23), in the frequency domain, the modal displacement of the system subjected to a unit amplitude ground acceleration $\ddot{u}_g\,(=\exp(i\omega t))$, is assumed to be

$$u = H_u(i\omega)\, e^{i\omega t} \tag{27}$$

and the acceleration as

$$\ddot{u} = -\omega^2 H_u(i\omega)\, e^{i\omega t} \tag{28}$$

Substituting equations (27) and (28) into equation (23), the following is obtained

$$[-\omega^2 M + K]H_u = -m \tag{29}$$

The unknown transfer function can be obtained from the above. And the transfer function for absolute acceleration is

$$H_{\ddot{u}} = -\omega^2 H_u + \delta \tag{30}$$

The shear strain and shear stress of the eth element are calculated in terms of $H_{ue}^{(1)}$ and $H_{ue}^{(2)}$, part of the solution vector H_u related to the eth element. The strain transfer function of the eth element is described as

$$H_{\gamma e} = \frac{H_{ue}^{(1)} - H_{ue}^{(2)}}{l_e}. \tag{31}$$

Utilizing the stress–strain relationship, the stress transfer function of the eth element is expressed

$$H_{\tau e} = G_e^* H_{\gamma e} \tag{32}$$

For the linear system, with the transfer function obtained from the proceeding calculation, the spectral density function of response can be obtained as

$$S_X(\omega) = \text{diag}\,[H_X(\omega)\, H_X^{*T}(\omega)]\, S_{\ddot{u}_g}(\omega) \tag{33}$$

where X is any random function, can be u, $\ddot{u}$ γ, or τ.

4.1.4. Statistical properties of extreme values. Let $X(t)$ be a stationary random functiom having a normal probability density function with zero mean and a power spectral density $S_X(\omega)$. The mean-square value of the process $X(t)$ in terms of its power spectral density is defined as

$$\sigma_X^2 = \int_{-\infty}^{\infty} S_X(\omega)\, \mathrm{d}\omega \tag{34}$$

The spectral moments about the origin are

$$\lambda_i = \int_{-\infty}^{\infty} \omega^i S_X(\omega)\, \mathrm{d}\omega, \quad i = 0, 2, 4 \tag{35}$$

The probability density function over a period T for normalized extreme values as obtained (Davenport, 1964) as

$$p_e(\eta) = vT \cdot \exp\left(\frac{-\eta^2}{2}\right) \cdot \exp\left(-vT \cdot \exp\left(\frac{-\eta^2}{2}\right)\right) \tag{36}$$

where $\eta = X/\sigma_X$ v is a measure of the most characteristc or predominat frequency in the function X and, is given as

$$v = \frac{1}{2\pi}\left(\frac{\lambda_2}{\lambda_0}\right)^{1/2} \tag{37}$$

Statistical properties of the random variable n, may be readily obtained once its probability density function is defined. Using equation (36) the mean, the mean square and standard deviation of the extreme values can also be obtained (Romo-Organista. 1977).

4.1.5. The equivalent liner methods. In the range of shear strains induced by strong earthquake motion, stress–strain behaviour of soil is significantly nonlinear with G and β being dependent on the level of strain. Idriss and Seed (1968) introduced an approximate equivalent linear methods of evaluating the seismic response, in which an approximate solutionis obtained by solving the linear system iteratively by using G and β compatible with the developed strain.

A set of initial modulus and damping ratio values are estimated for each soil element of the model. The mean-square value of mixmum sheat strain may be evaluated as described and then the mean of the extreme value $\hat{\gamma}_{\max}^0$ may be obtained. The effective shear strains are then computed by the following:

$$\hat{\gamma}_{\text{eff}} = 0{\cdot}65 \cdot E(\hat{\gamma}_n) = 0{\cdot}65\, \hat{\gamma}_{\max}^0 \tag{38}$$

New values of G and β compatible with effective strain, $\hat{\gamma}_{\text{eff}}$ are then read from experimentally generated curves. These values of G and β are then used in the next iteration of all the above

calculation steps, and the processes is repeated until convergence is achieved (usually withinh 3–5 iterations).

4.2. SFEM: Monte Carlo simulation

The direct Monte Carlo Simulation methods involves generating various realizations of the random field $\alpha(z)$ appearing in equation ((21) and evaluating the reponse with earh of these realizations separately. Finally, the statistics of these responses are evaluated.

Considering $\alpha(z)$ to be a zero mean, one-dimensional, and uni-variate real homogeneous random field the autocorrelation $R_{\alpha_0\alpha_0}(\zeta)$ and two-side spectral density function $S_{\alpha_0\alpha_0}(\kappa)$ can be written as

$$S_{\alpha_0\alpha_0}(\kappa) = \frac{1}{2\pi}\int_{-\infty}^{\infty} R_{\alpha_0\alpha_0}(\zeta)\, \mathrm{e}^{-\mathrm{i}\omega\zeta}\, \mathrm{d}\zeta \tag{39}$$

$$R_{\alpha_0\alpha_0}(\zeta) = \int_{-\infty}^{\infty} S_{\alpha_0\alpha_0}(\kappa)\, \mathrm{e}^{\mathrm{i}\kappa\zeta}\, \mathrm{d}\kappa \tag{40}$$

Based on Rice's (1954) suggested representation, the simulation $\alpha(z)$ of an 1d–1v stationary gaussian process with zero mean is expressed as

$$\alpha(z) = \sqrt{2}\sum_{j=1}^{n} \sqrt{2S_{\alpha_0\alpha_0}(\kappa_j)\,\Delta\kappa}\cos(\kappa_j z + \phi_j) \tag{41}$$

where

$$\kappa_j = j\Delta\kappa, \quad j = 1, 2, \ldots, n \tag{42}$$

ϕ_j are the phase angles distributed uniformly over the range $(0, 2\pi)$

The upper bound wave number is

$$\kappa_u = N\Delta\kappa \tag{43}$$

which represents an upper cut-off frequency beyond which $S_{\alpha\alpha}(\kappa)$ may be assumed to be zero.

4.3. SFEM: perturbation method

In this method, the functions and operators involved are expanded in a Taylor series about their repective mean values. In the following only a first-order perturbation is considered. Element stiffness, equation (25), can be written as

$$K_e = \frac{1}{l_e}\begin{bmatrix} 1 & -1 \\ -1 & 1 \end{bmatrix}(\bar{G}_e + \alpha_e)\,(1 + 2\mathrm{i}\beta) \tag{44}$$

Taking first two terms of the Taylor series expansion of K_e

$$K_e = K_e^0 + K_e^I\,\alpha_e \tag{45}$$

where

$$K_e^0 = K_e|_{\alpha_e=0} = \frac{\bar{G}_e}{l_e}\begin{bmatrix} 1 & -1 \\ -1 & 1 \end{bmatrix}(1+2\mathrm{i}\beta) \tag{46}$$

$$K_e^I = \left.\frac{\partial K_e}{\partial \alpha_e}\right|_{\alpha_e=0} = \frac{1}{l_e}\begin{bmatrix} 1 & -1 \\ -1 & 1 \end{bmatrix}(1+2\mathrm{i}\beta) \tag{47}$$

Global stiffness matrix, now becomes

$$K = K^0 + \sum_{i=1}^{N} K_i^I \alpha_i \tag{48}$$

4.3.1. Perturbation approximation for response. Using the above in equation (29), the equation of motion becomes

$$\left(K^0 + \sum_{i=1}^{N} K_i^I \alpha_i - \omega^2 M\right) H_u = -m \tag{49}$$

The above equation can be simplified as

$$DH_u = -m \tag{50}$$

with

$$D = K - \omega^2 M + \sum_{i=1}^{N} K_i^I \alpha_i \tag{51}$$

Taylor expansion of D, then yields

$$D = D^0 + \sum_{i=1}^{N} D_i^I \alpha_i \tag{52}$$

where

$$D^0 = K^0 - \omega^2 M \tag{53}$$

$$D_i^I = K_i^I$$

Transfer function in equation (50) can be solved as

$$H_u = D^{-1}(-m) = \left(D^0 + \sum_{i=1}^{N} D_i^I \alpha_i\right)^{-1}(-m) = H_u^0 + \sum_{i=1}^{N} H_{ui}^I \alpha_i \tag{54}$$

In which

$$H_u^0 = (D^0)^{-1}(-m) \tag{55}$$

$$H_{ui}^I = (-1)(D^0)^{-2}(D_i^I)(-m) = (D^0)^{-1}(-D_i^I H_u^0) \tag{56}$$

Similarly, the perturbation approximations for other variables such as acceleration, strain and stress can be computed. In the following $H_x(\mathrm{i}\omega)$ is used to represent the transfer function of any of these response variables. (57)

4.3.2. Perturbation approximation of spectral density of response. The spectral density function of a response variable, x can be obtained as

$$S_x = \text{diag}\,([H_x \cdot H_x^{*T}] \cdot S_{\ddot{u}_g}) \tag{58}$$

From equation (54)

$$H_x = H_x^0 + \sum_{i=1}^{N} H_x^I \alpha_i \tag{59}$$

Combining he above equations one can write

$$S_x = \text{diag}\left[\left(H_x^0 + \sum_{i=1}^{N} H_x^I \alpha_i\right)\left(H_x^{*0\mathrm{T}} + \sum_{i=1}^{N} H_x^{*\mathrm{IT}}\, \alpha_i\right)\right] S_{\ddot{u}_g} \tag{60}$$

Using the Taylor series expansion again

$$S_x = S_x^0 + \sum_{i=1}^{N} S_{xi}^I \alpha_i \tag{61}$$

Where

$$\begin{aligned} S_x^0 &= \text{diag}\,[H_x^0 \times H_x^{*\,\mathrm{OT}}]\, S_{\ddot{u}_g} \\ S_{xi}^{\mathrm{I}} &= \text{diag}\,[H_{xi}^0 \times H_{xi}^{*\,\mathrm{IT}} + H_{xi}^I \times H_x^{*\,\mathrm{OT}}]\, S_{\ddot{u}_g} \end{aligned} \tag{62}$$

Continuing along the same line, perturbation approximations can be obtained for the extreme values of the response variable.[24]

4.4. SFEM: spectral decomposition I

4.4.1. Karhunen–Loeve expansion and Neumann expansion. In this approach,[13] the random field $\alpha_G(z)$ is represented by Karhunen–Loeve expansion with an orthogonal decomposition

$$\alpha_G\,(z,\,\theta) = \sum_{k=1}^{m} \xi_k(\theta)\,\sqrt{\lambda_k}\,\phi_k(z) \tag{63}$$

where ξ_k are random coefficients and λ_k are the eigen values and the ϕ_k are the eigen functions of the autocorrelation function $R_{\alpha\alpha}(z)$

$$\xi_k = \frac{1}{\sqrt{\lambda_k}} \int_l \alpha_G\, \phi_k\, \mathrm{d}z \tag{64}$$

$$\int_l R_{\alpha\alpha}\,(z)\;\phi_k\,(z_2)\;\mathrm{d}z_2 = \lambda_k\;\phi_k(z_1) \tag{65}$$

while l is the thickness of the soil layer.

By the expansion in equation (63), the shear modulus in equation (21) becomes

$$G\,(z,\,\theta) = \bar{G}(z) + \sum_{k=1}^{m} \xi_k\,(\theta)\,\sqrt{\lambda_k}\;\phi_k(z) \tag{66}$$

In the above equation θ refers to the random character of the quantities involved.

4.4.2. Eigen value and eigen function of the autocorrelation function. With the autocorrelation function given by equation (22), the integral equation in equation (65) becomes

$$\sigma_G^2 \int_{-a}^{a} \mathrm{e}^{-c|z_1 - z_2|}\, \phi_k(z_2)\, \mathrm{d}z_2 = \lambda_k \phi_k(z_1) \tag{67}$$

where $c = 1/b$, $a = l/2$.

The solution of the above equation (25) is given by

$$\phi_k(z) = \frac{\cos(\omega_k z)}{\sqrt{a + \sin(2\omega_k a)/2\omega_k}} \quad \text{(for odd } k\text{)} \tag{68}$$

where ω_k are the solutions of

$$\tan \omega a - \frac{c}{\omega} = 0$$

$$\phi_k(z) = \frac{\sin(\omega_k z)}{\sqrt{a - \sin(2\omega_k^* a)/2\omega_k}} \tag{69}$$

and where ω_k are the solution of

$$\tan \omega a + \frac{\omega}{c} = 0 \tag{70}$$

The corresponding eigenvalues are

$$\lambda_k = \frac{2c}{\omega_k^2 + c^2}\, \sigma_G^2, \quad k = 1, 2, 3, \ldots \tag{71}$$

4.4.3. Finite element equation: spectral decomposition. In the finite element formulation with a linear shape function, the element stiffness matrix K_e can be written as

$$K_e = \bar{K}_e + \sum_{k=1}^{m} \xi_k K_{ek} \tag{72}$$

where

$$\bar{K}_e = \frac{\bar{G}(1 + 2\mathrm{i}\beta)}{l_e} \begin{bmatrix} 1 & -1 \\ -1 & 1 \end{bmatrix}$$

$$\bar{K}_{ek} = \frac{1 + 2\mathrm{i}\beta}{l_e} \sqrt{\lambda_k \phi_k} \begin{bmatrix} 1 & -1 \\ -1 & 1 \end{bmatrix} \tag{73}$$

while l_e is the height of the element.

The global stiffness matrix, K is obtained by assembling the element stiffness matrices over the entire region.

$$K = \sum_{e=1}^{N} K_e = \sum_{e=1}^{N} \bar{K}_e + \sum_{e=1}^{N} \sum_{k=1}^{m} \xi_k K_{eK}$$

$$= \bar{K} + \sum_{k=1}^{m} \xi_k K_k \tag{74}$$

where

$$K_k = \sum_{e=1}^{N} K_{ek} \tag{75}$$

Now, equation (29) can be written as

$$\left[-\omega^2 M + \bar{K} + \sum_{k=1}^{m} \xi_k K_k \right] H_u = -m \tag{76}$$

Let

$$D = -\omega^2 M + \bar{K} \tag{77}$$

and dividing both sides of the above equation by D then

$$\left[I + \sum_{k=1}^{m} \xi_k Q_k \right] H_u = f \tag{78}$$

where

$$\begin{aligned} Q_k &= D^{-1} K_k \\ f &= D^{-1} (-m) \end{aligned} \tag{79}$$

The solution of equation (78) is

$$H_u = \left[I + \sum_{k=1}^{m} \xi_k Q_k \right]^{-1} f \tag{80}$$

4.4.4. Response approximation: Neumann expansion. By improved Neumann expansion, the above equation can be expressed as

$$H_u = \left\{ \sum_{i=0}^{\infty} (-1)^i \left[\sum_{k=1}^{m} \xi_k Q_k \right]^i \right\} f \tag{81}$$

In the above equation, all the Q_k and f are known. After a series of operations on the matrix. The jth element of H_u, can be expressed as a function of $\xi_1, \xi_2, \ldots,$

$$\begin{aligned} H_{uj} = {} & (a_0 + a_1 \xi_1 + a_2 \xi_2 + a_3 \xi_1^2 + a_4 \xi_1 \xi_2 + a_5 \xi_2^2 + \cdots) \\ & + (b_0 + b_1 \xi_1 + b_2 \xi_2 + b_3 \xi_1^2 + b_4 \xi_1 \xi_2 + b_5 \xi_2^2 + \cdots)\, i \end{aligned} \tag{82}$$

4.4.5. Properties of ξ. ξ is a set of orthonormal uncorrelated Gaussian variables with the following properties:

$$\begin{aligned} &\langle \xi_i \rangle = 0 \\ &\langle \xi_i^2 \rangle = \delta_{ii} = 1 \\ &\langle \xi_i^{2n+1} \rangle = 0, \quad n = 1, 2, 3 \cdots \\ &\langle \xi_{\lambda_1} \cdots \xi_{\lambda_k} \rangle = \sum_{p=2}^{k} \langle \xi_{\lambda_1} \xi_{\lambda_p} \rangle \left\langle \prod_{m=2,\ m \neq p}^{k} \xi_{\lambda_m} \right\rangle \end{aligned} \tag{83}$$

Because ξ_i, ξ_j are independent, the mean values of the product can be expressed as

$$\langle \xi_i^m \, \xi_j^n \rangle = \langle \xi_i^m \rangle \, \langle \xi_j^n \rangle \tag{84}$$

4.4.6. Mean and variance of a response. A statistical property Y of a response variable viz., displacement can be expressed as a function of H_{uj} in equation (82). Of course, Y is the function of ξ also, that is

$$Y = g\,(\xi_1, \xi_2, \xi_3, \ldots, \xi_n) \tag{85}$$

Expanding the function g in the Taylor series about the mean values $u_{\xi_1}, \mu_{\xi_2}, \ldots, \mu_{\xi_n}$; in this case

$$Y = g\,(\mu_{\xi_1}, \mu_{\xi_2}, \ldots, \mu_{\xi_n}) + \sum_{i=1}^{n} (\xi_1 - \mu_{\xi_1}) \frac{\partial g}{\partial \xi_i} + \frac{1}{2} \sum_{i=1}^{n} \sum_{j=1}^{n} (\xi_i - \mu_{\xi_1})\,(\xi_j - \mu_{\xi_j}) \frac{\partial^2 g}{\partial \xi_i \, \partial \xi_j} + \cdots \tag{86}$$

where the derivatives are evaluated at $\mu_{\xi_1}, \mu_{\xi_2}, \ldots, \mu_{\xi_n}$. The second-order approximate mean of Y can be obtained as

$$E(Y) \approx g\,(\mu_{\xi_1}, \mu_{\xi_2}, \ldots, \mu_{\xi_n}) + \frac{1}{2} \sum_{i=1}^{n} \left(\frac{\partial^2 g}{\partial \xi_i^2} \right) \mathrm{Var}\,(\xi_i) \tag{87}$$

While the first-order variance of Y is

$$\mathrm{Var}\,(Y) \approx \sum_{i=1}^{n} \left(\frac{\partial g}{\partial \xi_i} \right)^2 \mathrm{Var}\,(\xi_i) \tag{88}$$

From the relationship among the transfer functions, equations (30–32) and following the equations (85)–(88), the first and second moment of the extreme values of any response variable can be obtained

4.5. SFEM: spectral decomposition II

4.5.1. Karhunen–Loeve expansion and polynomial chaos. In this approach,[14] K–L expansion is used as in the previous approach but instead of using the Neumann expansion, spectral expansion is made in terms of polynomial chaos.

Polynomal Chaos

The equation of motion (76) is

$$\left(-\omega^2 M + \bar{K} + \sum_{m=1} \xi_m K_m \right) H_u = -m \tag{89}$$

With $K_0 = -\omega^2 M + \bar{K}$, $\xi_0 = 1$, the above can be written as,

$$\left(\sum_{m=0} \xi_m K_m \right) H_u = -m \tag{90}$$

Expanding H_u by polynomial chaos, the jth element of H_u can be expressed as

$$H_{uj} = a_{j0}\Gamma_0 + \sum_{i_1=1}^{\infty} a_{ji_1}\,\Gamma_1\,[\xi_{i_1}] \sum_{i_1=1}^{\infty}\sum_{i_2=1}^{i_1} a_{ji_1i_2}\,\Gamma_2\,[\xi_{i_1}\,\xi_{i_2}] \tag{91}$$

$$+ \sum_{i_1=1}^{\infty}\sum_{i_2=1}^{i_1}\sum_{i_3=1}^{i_2} a_{i_1i_2i_3}\,\Gamma_3\,[\xi_{i_1}\,\xi_{i_2}\,\xi_{i_3}] + \cdots \tag{92}$$

where $\Gamma_p\,[\ ]$ is the polynomial chaos of order p, and is given by the expression

$$\Gamma_p\,[\xi_{i_1}\,\xi_{i_2}\cdots\xi_{i_n}] = \frac{(-1)^n}{\mathrm{e}^{(-1/2)\xi\xi^{\mathrm{T}}}}\left[\frac{\partial_n}{\partial\xi_{i_1}\,\partial\xi_{i_2}\cdots\partial\xi_{i_n}}\,\mathrm{e}^{(-1/2)\xi\xi^{\mathrm{T}}}\right] \tag{93}$$

where $\xi\beta$ = vector of random variables $\{\xi_{i_1}, \xi_{i_2}, \ldots, \xi_{i_n}\}$.

The polynomial chaos of order greater than one have zero mean value, and polynomials of different order are orthogonal to each other.

After expanding the summation in equation (92), the H_{nj} can also be expressed in the form of

$$H_{uj} = \sum_{i=0}^{P} c_{ji} r_i \tag{94}$$

where P is the number of polynomial chaos, excluding the zeroth order term.

Equation (94) is still a function of polynomial chaos, and there is a one-to-one relationship between the coefficients a in equation (92) and the coefficient c in equation (94). Combining equation (90) and (94), we get

$$\left(\sum_{m=0}^{M} \xi_m K_m\right)\left(\sum_{i=0}^{P} c_{ni} r_i\right) = -m \tag{95}$$

Multiply both sides of equation (95) by r_i, $i = 0 \cdots P$, and taking the expected value, we get

$$KC = F \tag{96}$$

where

$$K_{ij} = \sum_{m=0}^{M} K_m\,\langle r_i r_j \xi_m\rangle, \quad i,j = 0,\ldots,P$$

$$F_i = \langle -mr_i\rangle, \quad i = 0,\ldots,P$$

$$F_i = -m \quad \text{for } i = 0$$

$$F_i = 0 \quad \text{for } i \neq 0 \tag{97}$$

K is a $N(P+1)\times N(P+1)$ matrix, C and F are $N(P+1)$ arrays.

From equation (96) we can get C, With C back in equation (94), ,we will have H_{uj}.

$$S_{un} = (H_{un} \times H^*_{un})\,S_{\ddot{u}_g} = A_{un}\,S_{\ddot{u}_g} \tag{98}$$

$$\langle A_{un}\rangle = \sum_{i=0}^{P} c_{ni}^2 \times \langle r_i^2\rangle \tag{99}$$

The tables provided in Spanos and Ghanem[13] are used to make the calculations in the above. H_{un} can also be expressed as a function of $\xi_1, \xi_2, \ldots$, as was done in equation (82). The rest of the procedure will be the same as equation (85)–(88) in the previous section.

5. NUMERICAL RESULTS

5.1. An example problem

Four stochastic finite element methods for the analysis of seismic response of sites are applied to study the site at Kawagishi–Cho which suffered severe liquefaction during the Niigata earthquake of 16 June 1964. This case has been studied extensively, and a significant amount of information is available on the properties of the *in situ* saturated sand deposits. The numerical

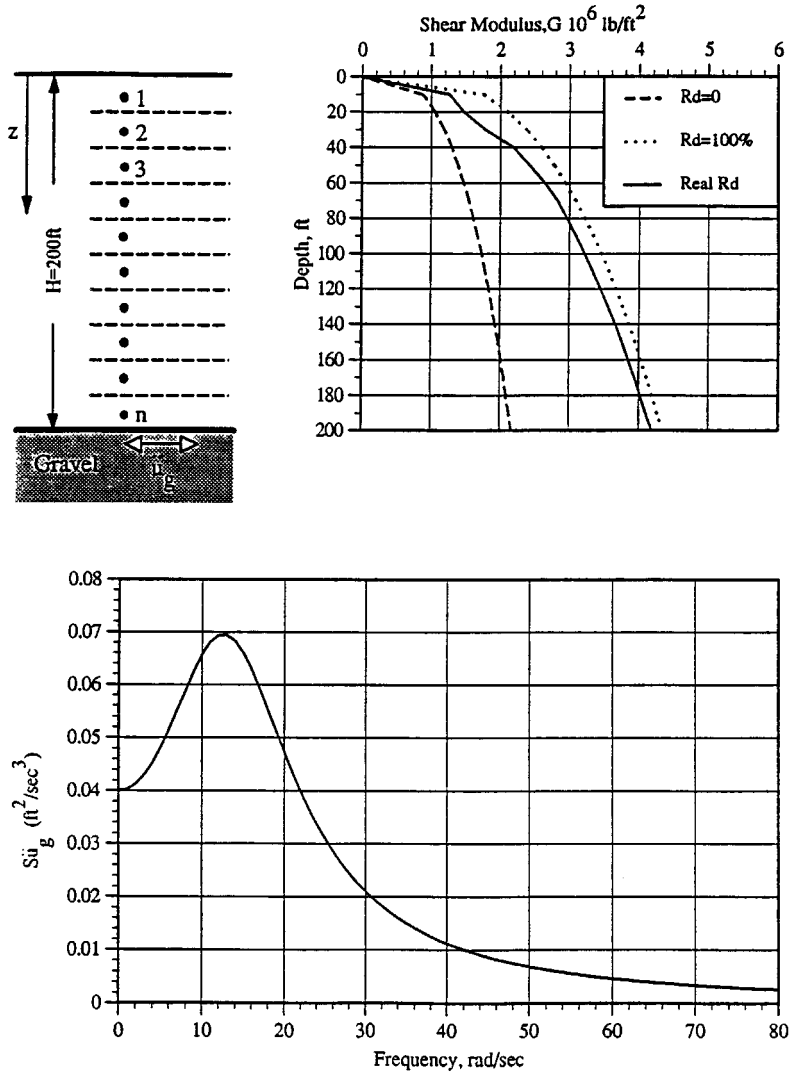

Figure 3. Soil conditions and power spectral density of ground motion—Niigata earthquake, 1964

results obtained from different methods are compared with respect to accuracy and computing efficiency.

5.1.1. Parameters of seismic excitation. The ground motions developed at Niigata were generated by an earthquake of magnitude, M_e, about 7·3, at an epicentral distance, R, of about 35 miles (56 km). Based on the strong motion, the accelerogram in the basement of the apartment building

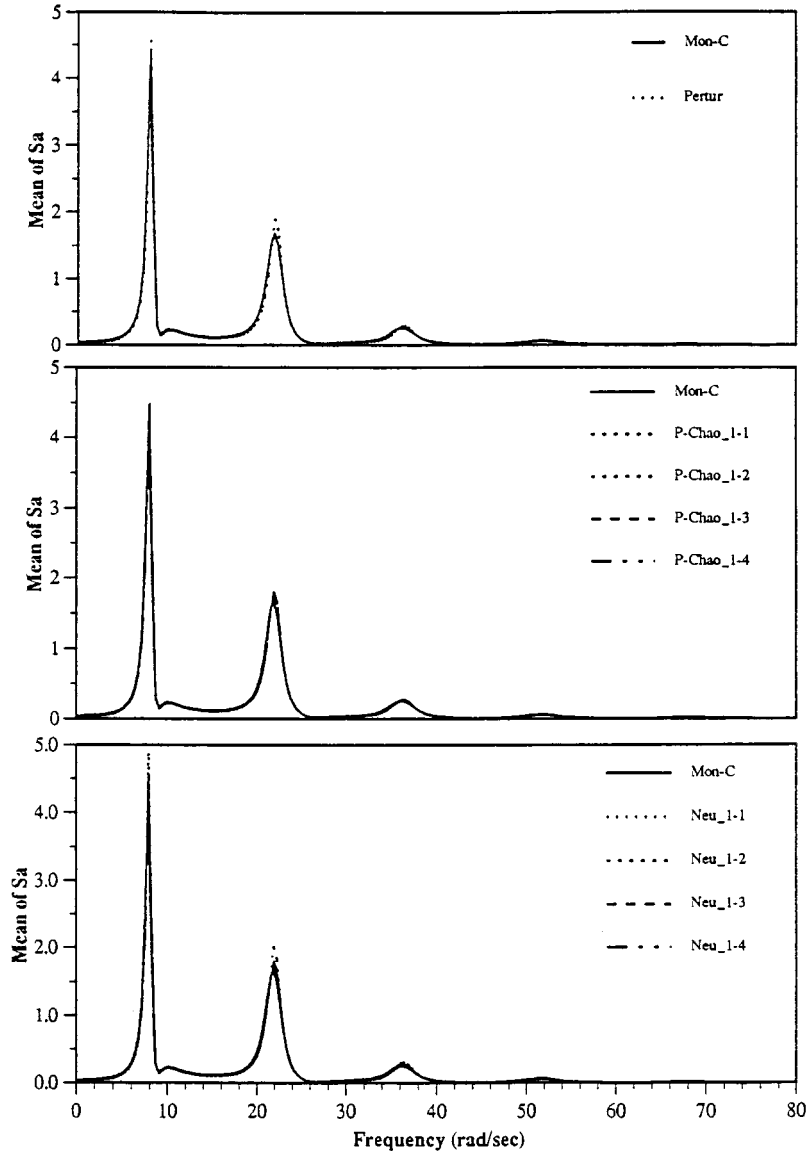

Figure 4. Mean value of acceleration power spectrum density (Sa) ($\delta = 20$ ft, C.O.V. of $G = 0{\cdot}1$, iteration = 0)

No. 2 at Kawagishi–Cho recorded, the duration of the earthquake, s, and the duration of the strong portion of the accelerogram, t_l, as 26 s and 8 s, respectively. From the equations presented in Section 2, we can calculated the following parameters:
The expected maximum acceleration,

$$E[\ddot{u}_{g_{\max}}] = 1230\,e^{0{\cdot}8M_e}\,(R+25)^{-2} = 64{\cdot}45\ \mathrm{cm/s^2} = 2{\cdot}11\ \mathrm{ft/s^2}. \tag{100}$$

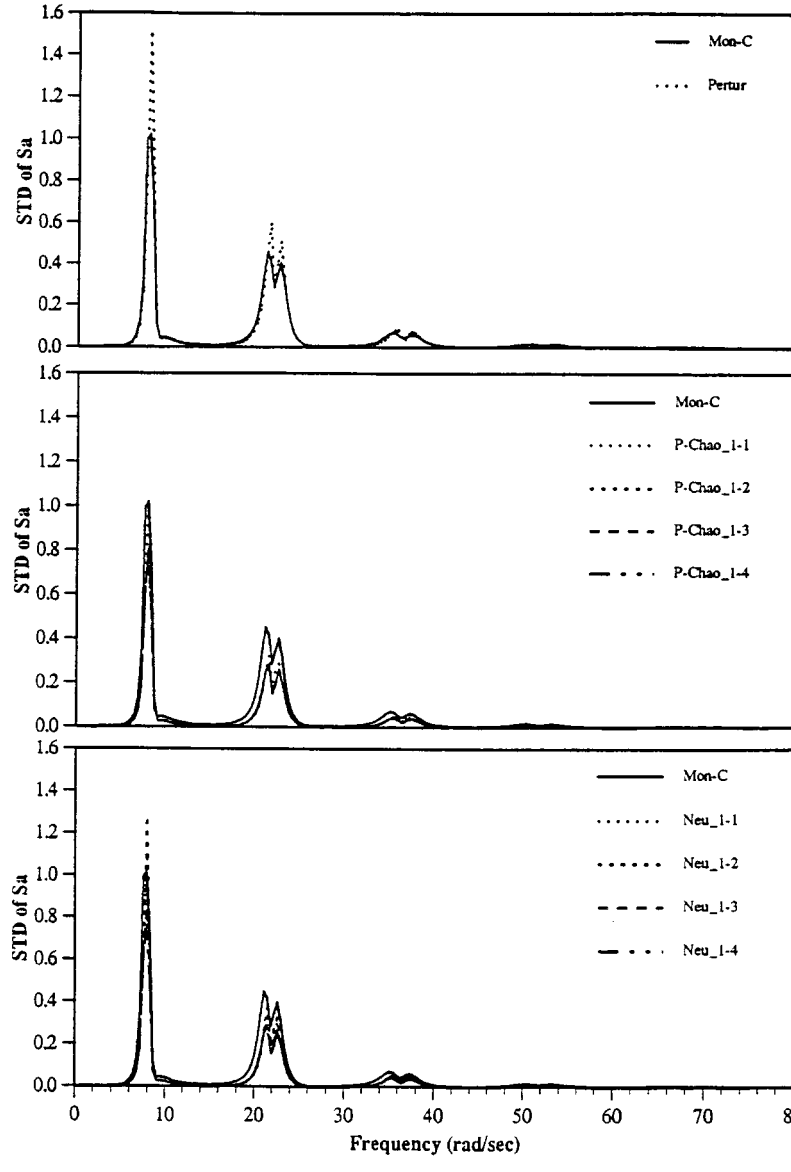

Figure 5. Standard deviation of acceleration power spectrum density (Sa) ($\delta = 20$ ft, C.O.V. of $G = 0{\cdot}1$, iteration $= 0$)

The expected highest peak acceleration

$$\ddot{u}_{g\max} = E\,[\ddot{u}_{g\max}] \cdot \Delta_{\ddot{u}_g} = 2{\cdot}11 \times 2{\cdot}05 = 4{\cdot}33\ \mathrm{ft/s^2}. \tag{101}$$

The coefficient of equivalent duration,

$$c_0 = 0{\cdot}25 + 0{\cdot}75\, t_l/s = 0{\cdot}25 + 0{\cdot}75 \times 8/26 = 0{\cdot}4808 \tag{102}$$

The standard deviation of acceleration

$$\sigma_{\ddot{u}_g} = \ddot{u}_{g\max}\,[2 \ln (2c_0 s/T_a)] = 1{\cdot}41\ \mathrm{ft/s^2} \tag{103}$$

The Kanai–Tajimi spectral density function is used to characterize the frequency content of the input ground acceleration with the natural frequency of ground, $\omega_g = 15{\cdot}56$ rad/s, and the damping ratio, $\zeta_g = 0{\cdot}64$. The scale factor, S_0, is calculated,

$$S_0 = \frac{4\zeta\,\sigma^2_{\ddot{u}_g}}{\pi\omega_g\,(1 + 4\zeta_g^2)} = \frac{4 \times 0{\cdot}64 \times 1{\cdot}41^2}{\pi \times 15.56 \times (1 + 4 \times 0{\cdot}64^2)} = 0{\cdot}039\ \mathrm{ft^2/s^3} \tag{104}$$

The spectral density of the input ground motion developed from the above parameters are shown in Figure 3.

5.1.2. Soil properties. In the case of the soil deposit at Niigata, it is known that the total depth to relatively firm base material is about 200 ft. The upper 100 ft is essentially sand, and the lower

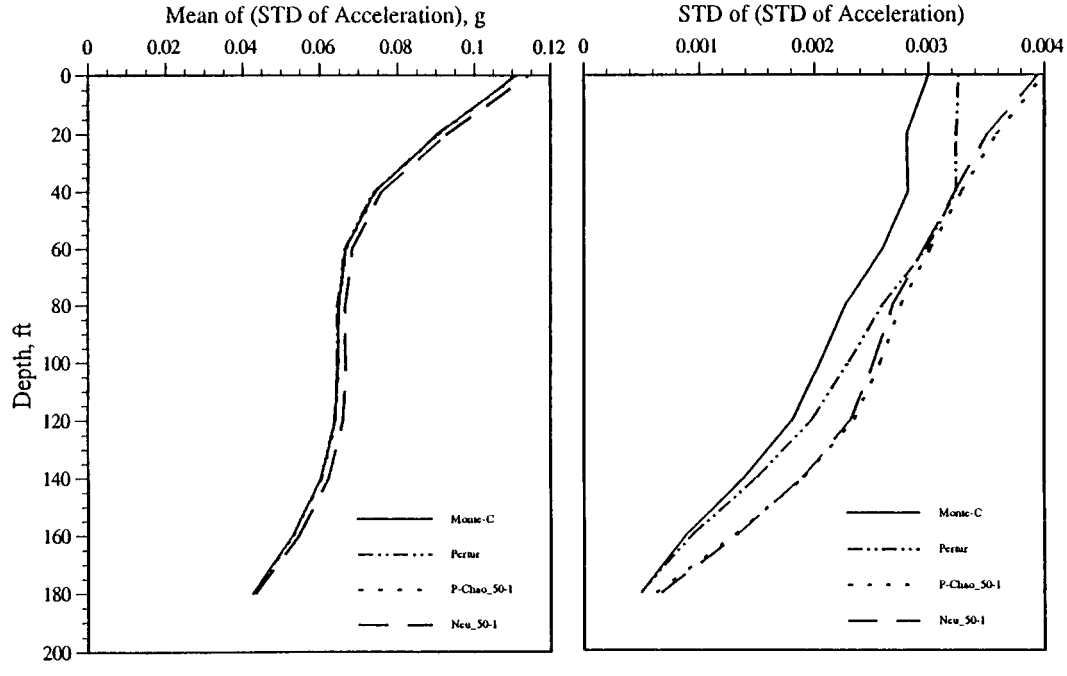

Figure 6. Comparison of mean values of STD of (STD of acceleration) (iteraction = 0)

100 ft is either stiff clay or clayey sand. Because the shear moduli of sand and stiff clays do not differ greatly, for practical purposes, the deposit may be considered to consist of sand throughout the full depth.

For the vibration amplitudes likely to develop during earthquakes, the moduli are likely to be around $G = 1 \times 10^5 \times \sigma_0^{1/3}$ psf for very loose sands, or $G = 2 \times 10^5 \times \sigma_0^{1/3}$ psf for very dense sand, in which σ_0 is the overburden pressure in pounds per square foot. If it is assumed that the above values are applicable for sands with relative density 0 and 100 per cent, respectively, then appropriate values of the shear modulus for sand at any relative density can be estimated by interpolation.

The relative density is about 45 per cent in the top 10 ft, dropping to about 40 per cent at a depth of 20 ft, and then increasing again to a relative density of about 80 per cent at a depth of

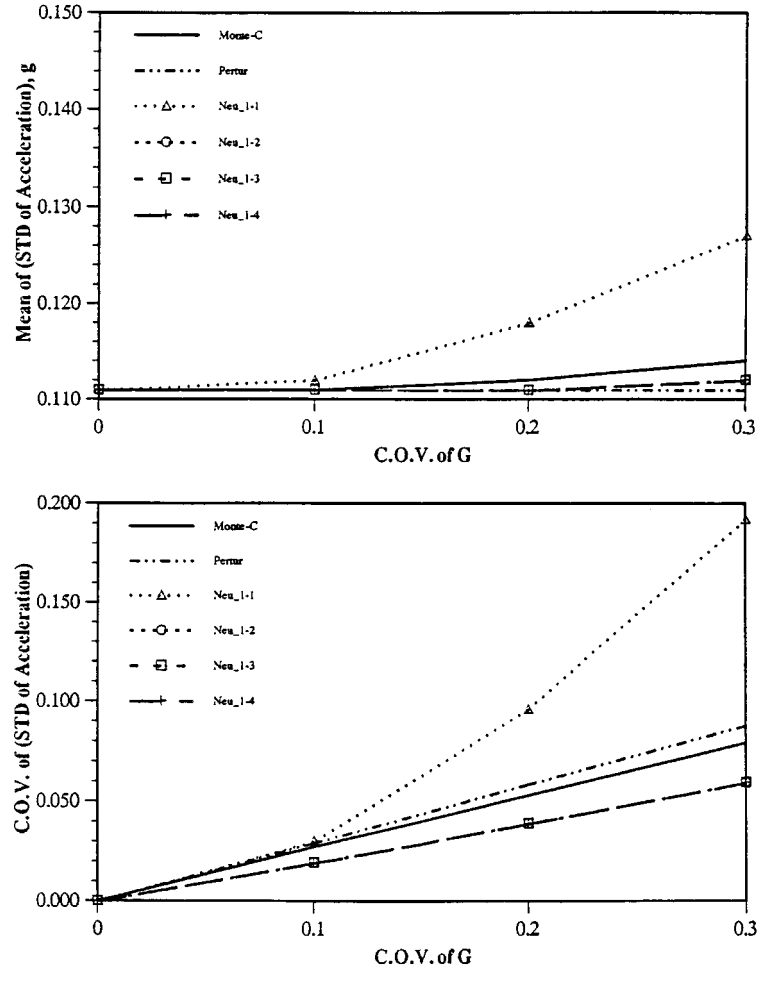

Figure 7. Mean and C.O.V. of the standard deviation of acceleration on ground surface for $\delta = 20$ ft; Neumann expansion with order of K–L expansion = 1 (iteration = 0)

60 ft. For the purpose of the analyses, it has been assumed that the relative density is between 80 and 90 per cent in the lower 130 ft of the deposit.

In the heavy damage zone in Niigata the water table is typically about 3 ft below the ground surface. Assuming that the unit weight of the sand above the water table is 110 lb/ft^3, and the buoyant weight below the water table is 50 lb/ft^3, the overburden pressures can readily be computed and the corresponding shear moduli determined from the above. The moduli determined in this way are plotted in Figure 3. According to the available experimental data on the damping ratio of sand, a value of $\beta = 0{\cdot}04$ is used. The variability of the shear modulus of sand is assumed to be characterized by the standard deviation $\sigma_G = 0{\cdot}1\ G$ and the scale of fluctuation, $\delta_G = 20$ ft.

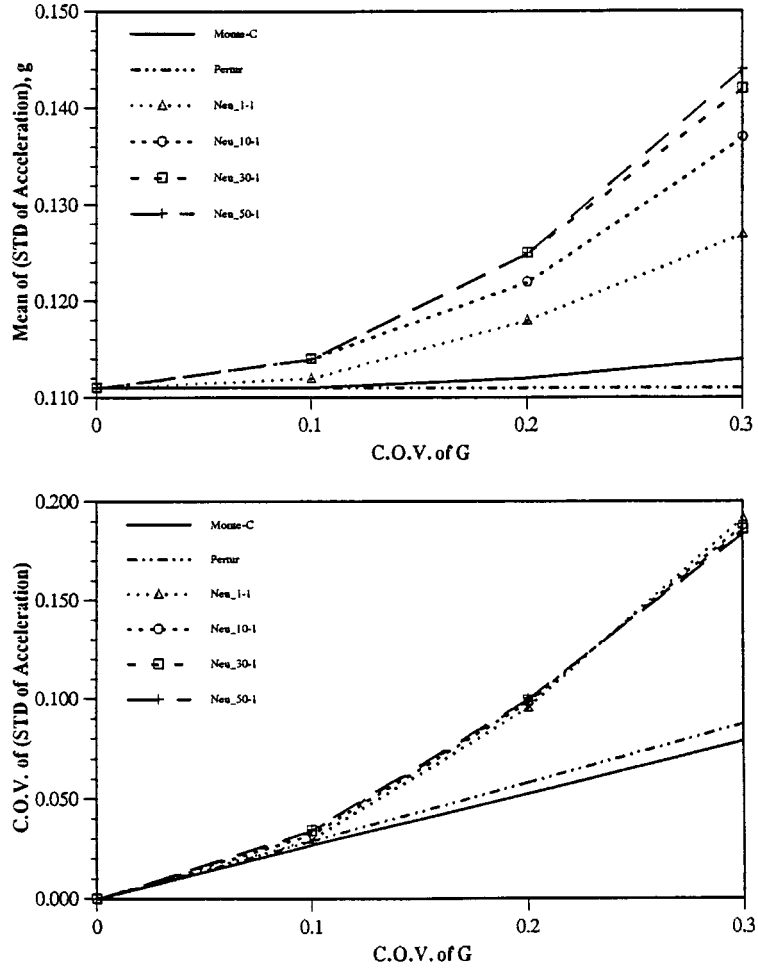

Figure 8. Mean and C.O.V. of the standard deviation of acceleration on ground surface for $\delta = 20$ ft; 1st order neumann expansion with K–L expansion (iteration = 0)

5.2. Results and discussion

In the following, the numerical results of seismic response obtained from stochastic finite element methods are compared with those from the Monte-Carlo simulation which is considered the most reliable method of analysis. In the figures referred below, the notation of the Neumann expansion and polynomial chaos are followed by the two digits; the first digit represents the order of the Karhunen–Loeve expansion, while the second one represents the order of the Neumann expansion or Polynomial Chaos.

Figure 4 presents the comparison of the mean values of the acceleration response power spectrum, $S_{\ddot{u}}$, on the ground surface, while Figure 5 shows the comparison of standard deviations of $S_{\ddot{u}}$ on the ground surface. In these figures the results from the polynomial chaos method match

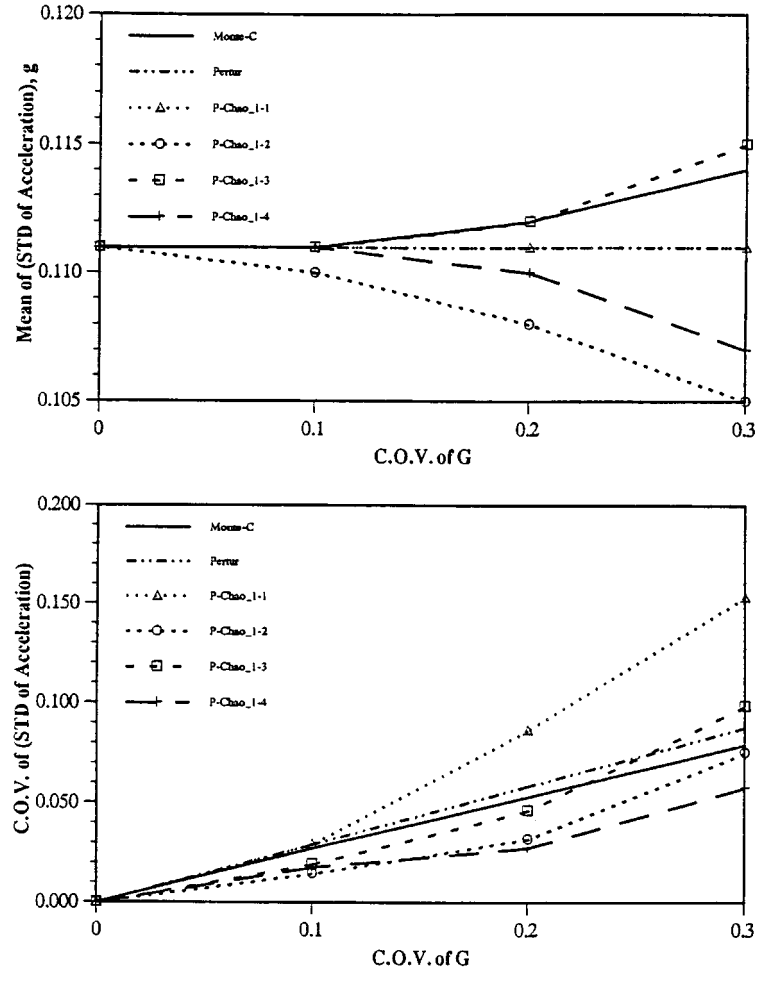

Figure 9. Mean and C.O.V. of the standard deviation of acceleration on ground surface for $\delta = 20$ ft; Polynomial chaos with order of K–L expansion = 1 (iteration = 0)

well to those of simulation, while the results from the perturbation method and the Neumann expansion tends to become larger at the natural frequencies, with the increase in the order of expansion.

Figure 6 shows the mean and standard deviation values of, $\sigma_{\ddot{u}}$, along the soil profile, with the C.O.V. of $G = 0{\cdot}1$. In these cases, the order of Karhunen–Loeve expansion is 50, and order of the Neumann expansion or polynomial chaos is 1. These figures indicate that mean values obtained by each method are almost the same. The results of standard deviation from the perturbation methods are always better than those from polynomial chaos or the Neumann expansion.

Figure 7 presents the mean and coefficient of variance of $\sigma_{\ddot{u}}$, on the ground surface considering the effect of variance of the C.O.V. of G, while the scale of fluctuation is 20 ft. The order of the

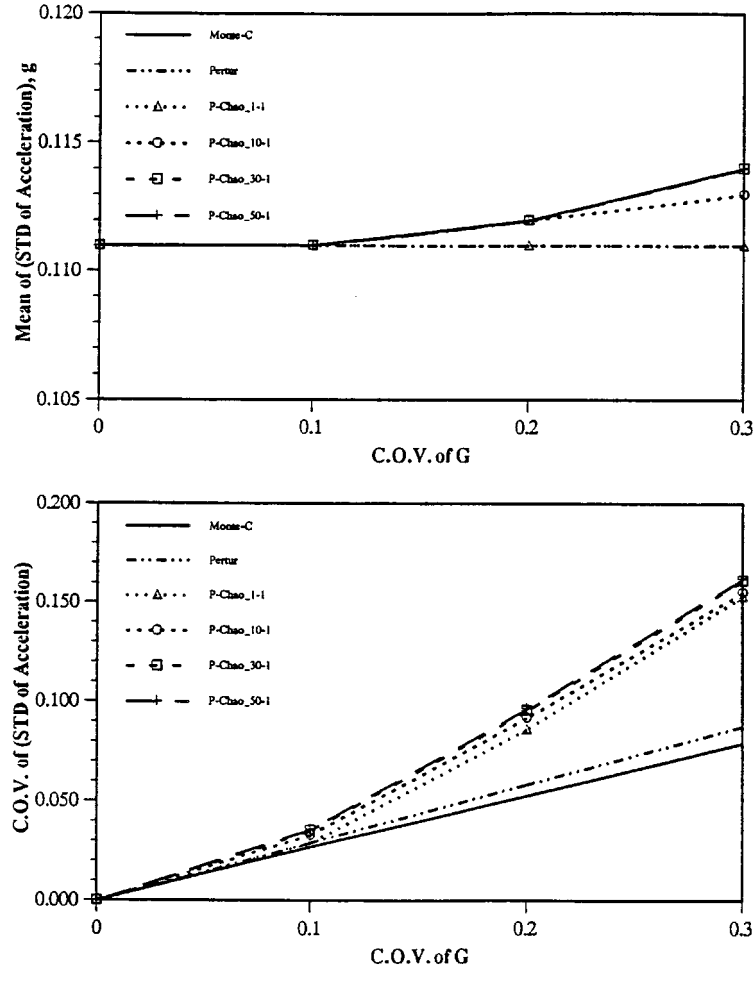

Figure 10. Mean and C.O.V. of the standard deviation of acceleration on ground surface for $\delta = 20$ ft; First order polynomial chaos with K–L expansion (iteration = 0)

Karhunen–Loeve is 1, and order of the Neumann expansion are from 1 to 4. It is noted that, in the case of the order of K–$L = 1$, using Neumann expansion higher than 2 does not change the result. For the first-order perturbation method, the mean value of response of the function of the mean of G, so it remains constant with the change of the C.O.V. of G. Figure 8 is similar to Figure 7, but the orders of the Karthunen–Loeve expansion are 1, 10, 30 and 50, and the order of the Neumann expansion is 1. Similar results, using the method of polynomical chaos, are presented in Figures

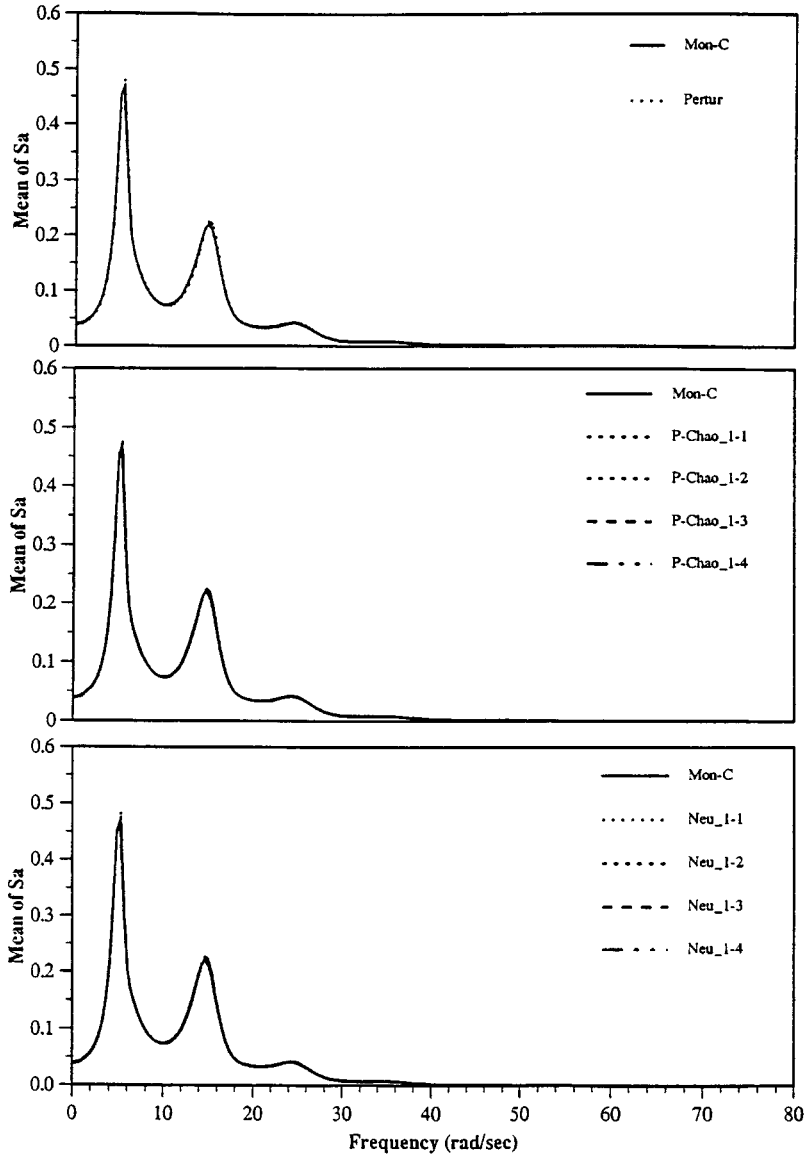

Figure 11. Mean value of acceleration power spectrum density (Sa) ($\delta = 20$ ft, C.O.V. of $G = 0{\cdot}1$, iteraction = 6)

9 and 10. In these cases, the performance of the lower order Karhunen–Loeve expansion is better than the higher one. It can be observed that the C.O.V. of σ_{ii} from the Neumann expansion and polynomial chaos converge to values different from the Monte-Carlo simulation results.

Figures 11–13 present the other set of results, for which soil properties are considered to be non-linear, and six iteractions are used. Since the equivalent linear method uses the obtained shear strain to determine the initial shear modulus and damping ratio for the next iteration, the

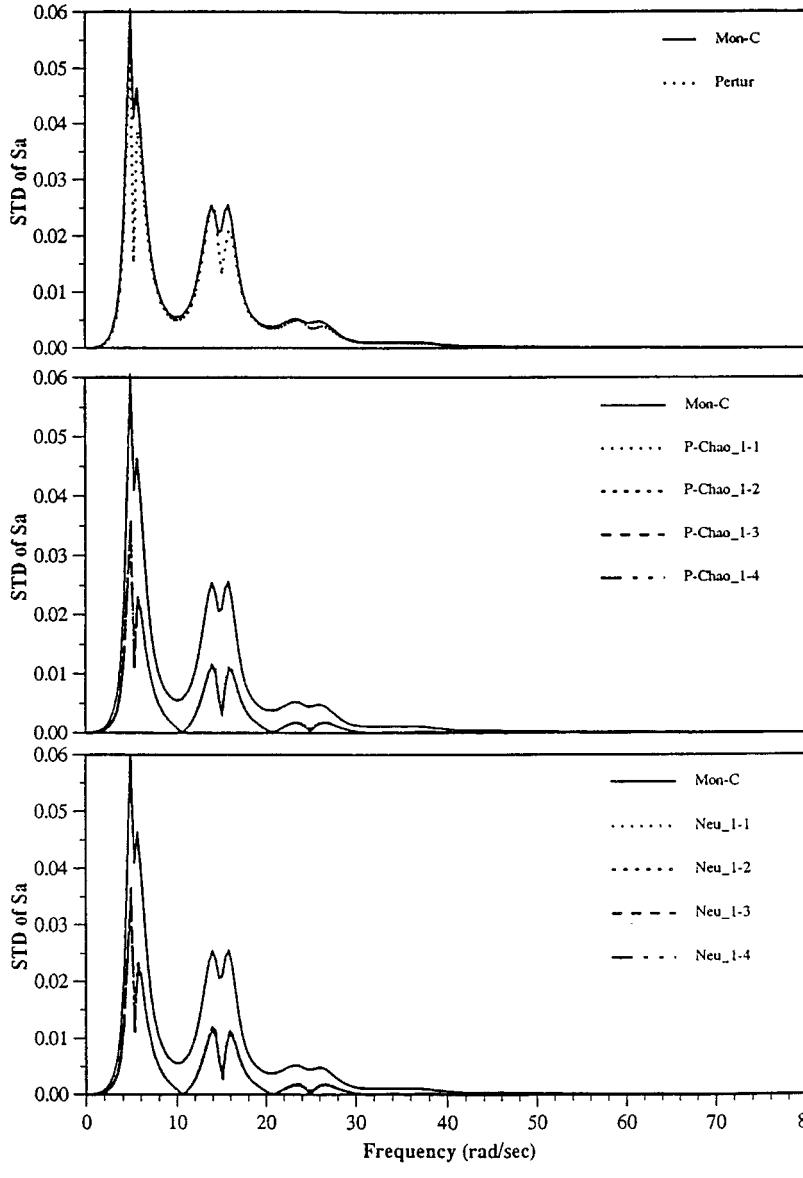

Figure 12. Standard deviation of acceleration power spectrum density (Sa); ($\delta = 20$ ft, C.O.V. of $G = 0{\cdot}1$, iteraction $= 6$)

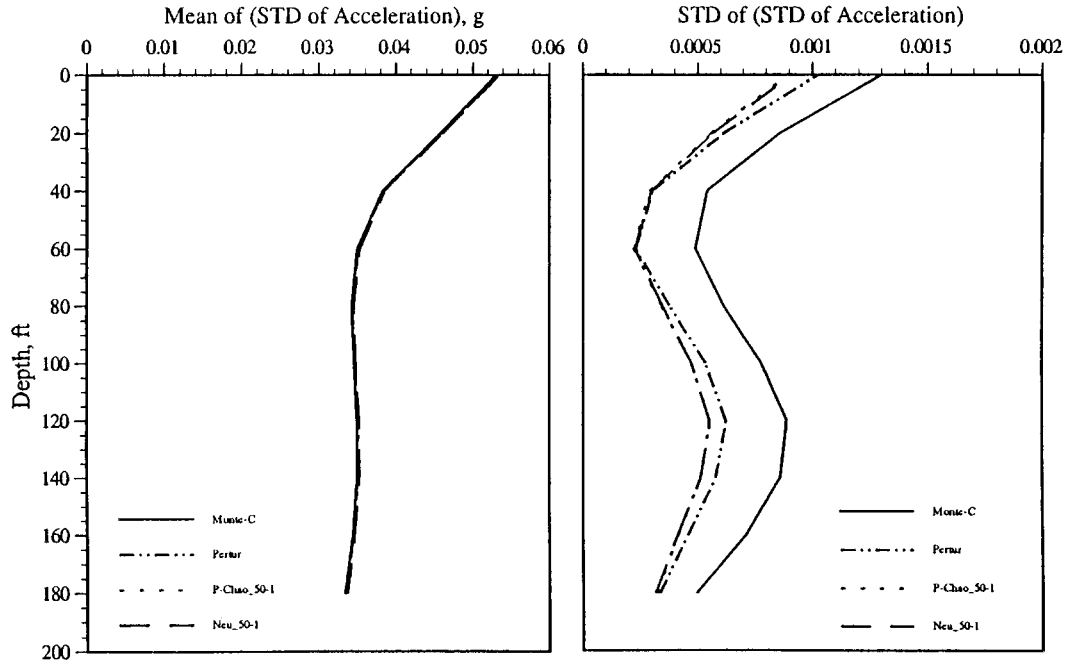

Figure 13. Comparison of mean values and STD of (STD of acceleration) (iteration = 6)

error is cumulative. The results of polynomial chaos and the Neumann expansion get worse compared to the linear case.

The CPU times used in DEC station 5100 for each method, without iteration, are shown in Figure 14. The run time for simulation is proportional to the sample size. For the spectral decomposition methods, the run time has been found to be almost proportional to the order of K–L expansion used. The perturbation method is computationally the most efficient method among these methods, while the simulation is the least efficient.

In order to understand the difficulties associated with K–L expansion based methods, the approximations of the covariance surfaces generated by various methods are examined. Figure 15 shows a target covariance surface which is approximated by various methods. Figure 16 shows the covariance surfaces approximated by Monte-Carlo simulation. Figures 17 and 18 show the results from the K–L expansion with two and five terms. Figures 19 and 20 shows the approximated surfaces for a large domain with 10 terms and 50 terms K–L expansion. It should be noted that the Monte-Carlo simulation provides a very good approximation. K–L expansion for smaller domains also yields a good approximation with five terms. However, for the larger domain, K–L expansion requires much larger number of terms for a reasonably good approximation. This shows that the convergence speed of K–L expansion depends on the relation between b and a. When the length of the domain is large compared to the correlation length, then a much higher order of K–L expansion is needed to achieve a good approximation. Unfortunately, this is the case for a typical soil profile. With the increase in order of K–L expansion, the number of the terms in the Neumann expansion, or polynomial chaos, increases rapidly. This makes the

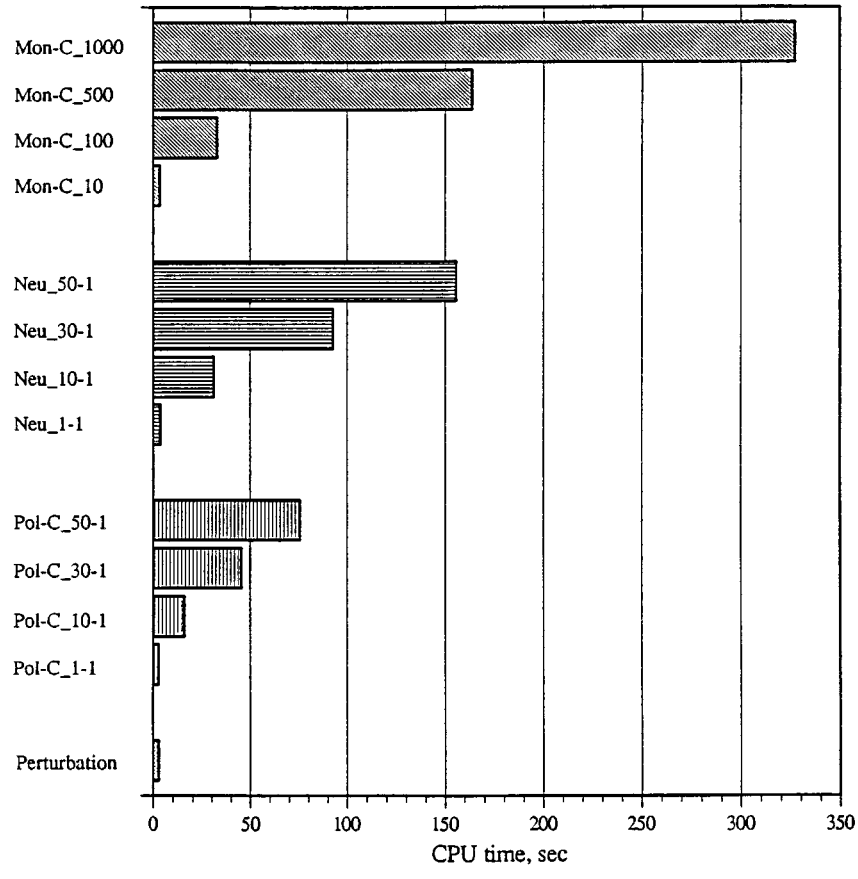

Figure 14. Comparison of CPU time

calculation for reasonably accurate results unfeasible or, at least, inefficient when compared to Monte-Carlo simulation.

From other results, we find that, if the problem is limited to finding the transfer functions, then even with a large variance of shear modulus, polynomial chaos will give reasonably good results, at least better than those produced by the perturbation method. However, it is not suitable to use polynomial chaos for further calculations, such as for the evaluation of non-linear functions of the transfer function. Every step of the operation on functions means a more complicated polynomial to deal with and will inevitably produce more error.

5.3. Closure

In this paper stochastic finite element methods are adapted and evaluated for the analysis of seismic response of soils. The uncertainties associated with both the seismically induced ground motion and the stiffness characteistics of the soil are considered.

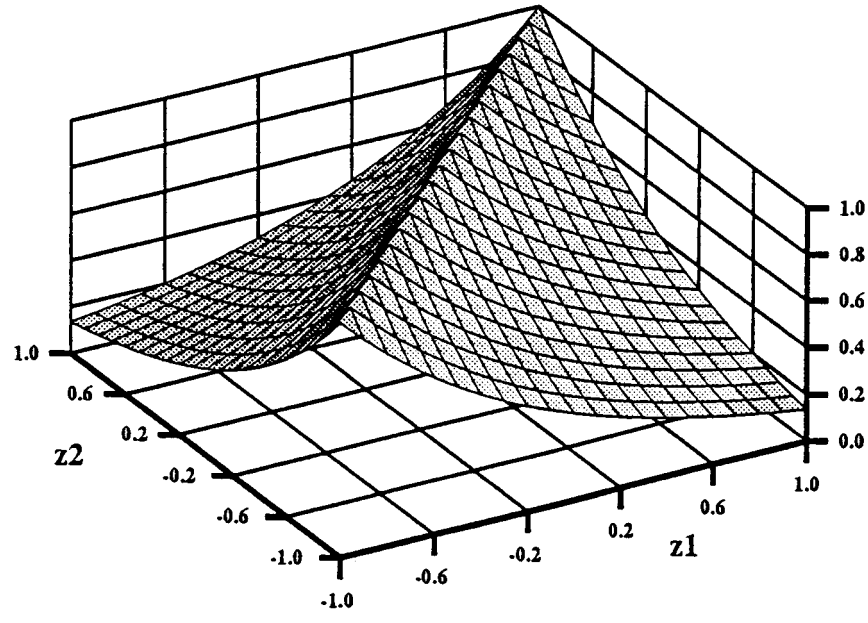

Figure 15. Exact covariance surface versus locations z1 and z2; Correlation length, $b = 1Z$

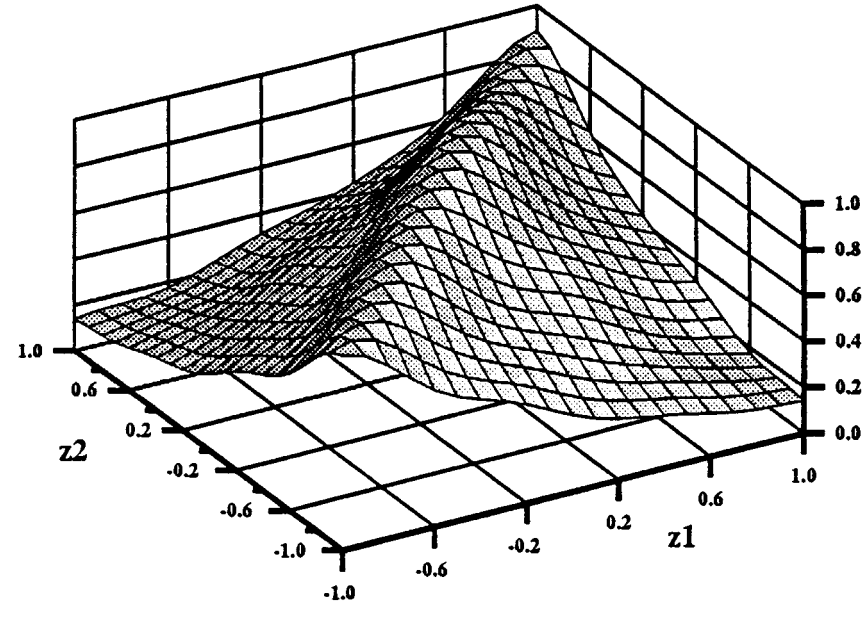

Figure 16. Covariance surfface versus locations z1 and z2 with Monte-Carlo simulation; correlation length, $b = 1$

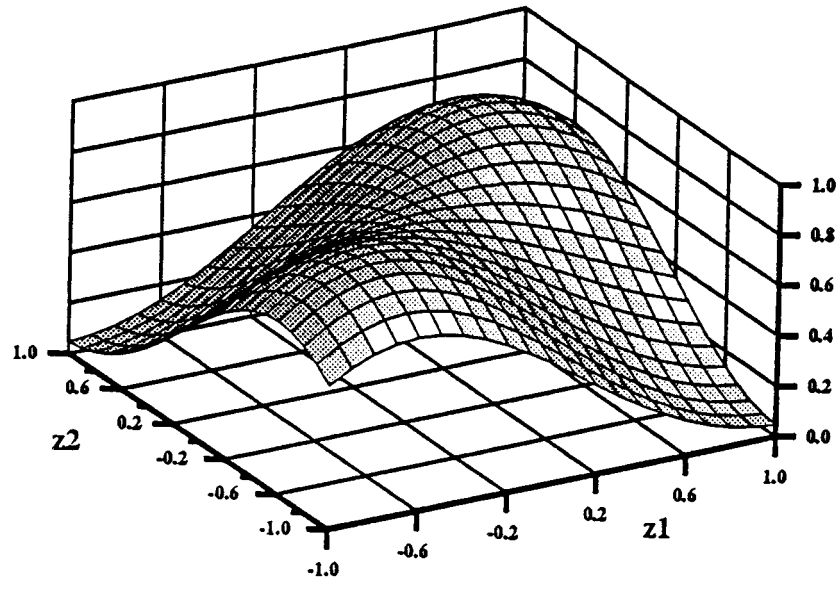

Figure 17. Covariance surface versus locations z1 and z2 with 2-term Karhunen–Loeve expansion; correlation length, $b = 1$; length of domain, $2a = 2$

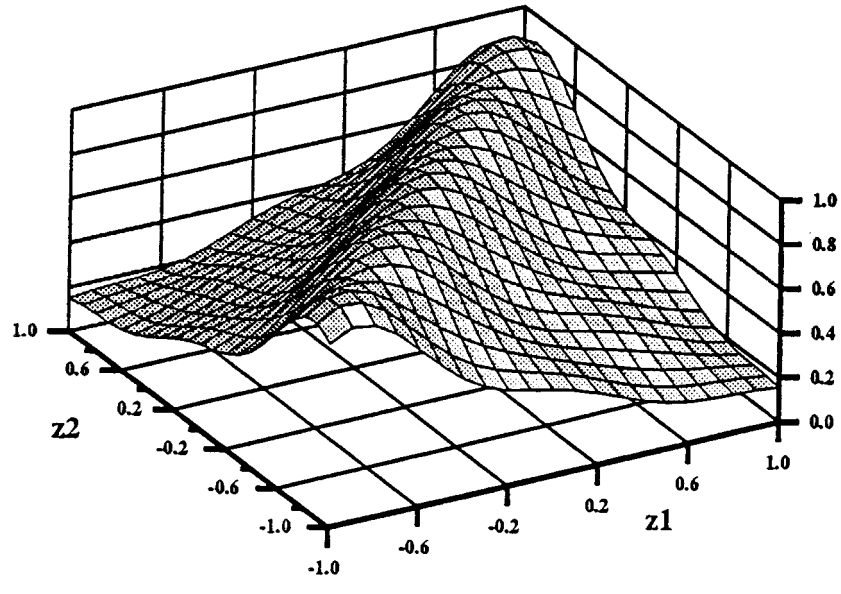

Figure 18. Covariance surface versus locations z1 and z2 with 5-term Karhunen–Loeve expansion; correlation length, $b = 1$; length of domain, $2a = 2$

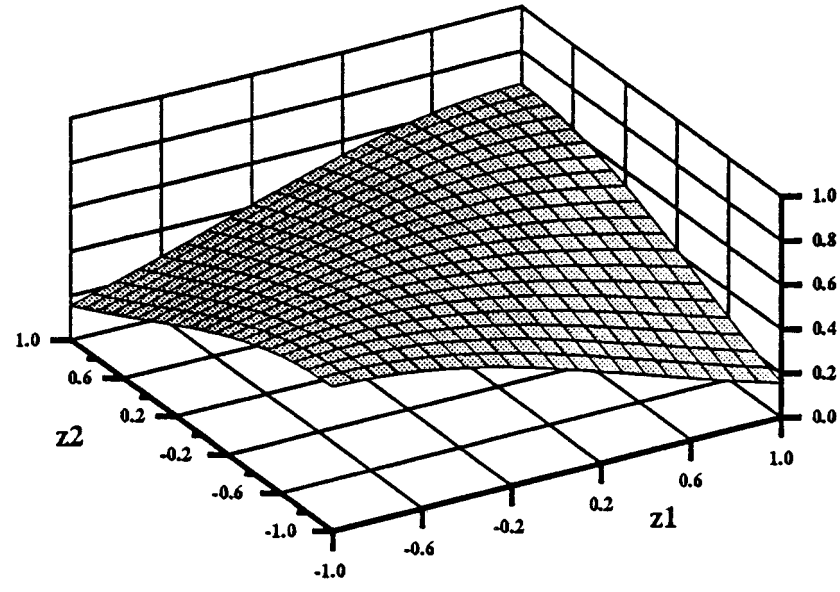

Figure 19. Covariance surface versus locations z1 and z2 with 10-term Karhunen–Loeve expansion; correlation length, $b = 1$; length of domain, $2a = 20$

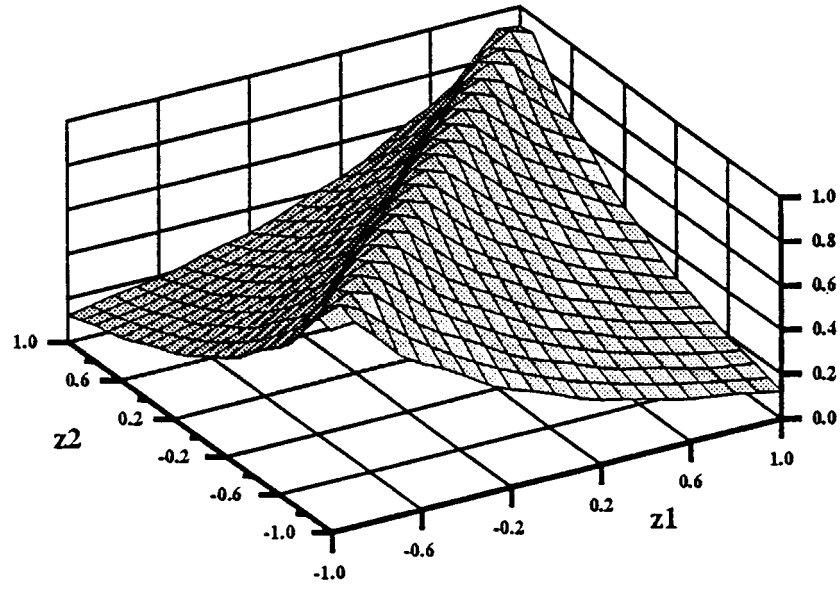

Figure 20. Covariance surface versus locations z1 and z2 with 50-term Karhunen–Loeve expansion; correlation length, $b = 1$; length of domain, $2a = 20$

Four available methods of stochastic finite element analysis considered here are: (i) Monte-Carlo simulation, in which many numerical realizations of the random field is generated, the response for each of the realizations is obtained by the solving the deterministic equation, and the variability of the response is evaluated from the statistics of the response; (ii) perturbation methid in which the random component of all the functions and operators are expanded through the Taylor series about their mean values, and with the first few terms of the series, the response is evaluated from the properties of the random components; (iii) spectral decomposition with Neumann expansion, then first the random field is represented by means of Karhunen–Loeve expansion, then the resulting algebraic equations are solved by the Neuman expansion of the inverse matrix, and (iv) spectral decomposition with polynomial chaos, where Karhunen–Loeve expansion is still used as in the previous method while the solution of the response is obtained using an approximation of the basis of poloynomial chaos.

The comparative study of these stochastic finite element methods, presented here, shows that a direct Monte-Carlo simulation is the most reliable stochastic finite element method for the analysis of seismic response of soils. Other methods specially spectral decomposition methods are mathematically quite complicated and do not always yield good results.

REFERENCES

1. A. G. Franklin and F. K. Chang, 'Earthquake resistance of earth and rock-fill dams: permanent displacement of earth embankments by newmark sliding block analysis', *Misc. Paper 5-71-17*, Dept. 5, U.S. Army Engineer Waterways Experiment Station, Viesburg, 1977.
2. M. P. Romo-Organista, 'Soil-structure interaction in a random seismic environment, *Ph.D. Dissertation*, Department of Civil Engineering, University of California, Berkeley, 1977.
3. G. Deodatis and M. Shinozuka, 'Stochasic FEM analysis of a wave propagation problem', *Technical Report*, Columbia University, 1987.
4. T. Igusa and A. D. Kureeghian, 'Response of uncertain systems of stochastic excitations', *J. Engng. Mech. ASCE*, **114** (EM5) 812–832 (1988).
5. G. B. Baecher, and T. S. Ingra, 'Stochastic FEM in settlement predictions', *J. Geotech. Eng. Div. ASCE*, **107** (GT4), 449–463 (1981).
6. G. Righetti and K. Harrop-Williams, 'Finite element analysis of random soil media', *J. Geotech. Eng. ASCE*. **104** (1), 59–75 (1988).
7. M. Shinozuka, 'Monte Carlo solultion of structural dynamics', *Int. J. Comput. Struct*., **2,** 855–874 (1972).
8. M. Shinozuka, 'Structural response variability', *J. Engng. Mech, ASCE*, **113** (EM6), 825–842 (1987).
9. T. Hisada and S. Nakagiri, 'Role of stochastic finite element method in structural safety and reliability', *Proc. 4th Int. Conf. on Structural Safety and Reliability*, Kobe, Japan, 1985, pp. 1385–1394.
10. W. K. Liu, T. Belytschko and A. Mani, 'Probabilistic finite elements for nonlinear structural dynamics', *Comput. Meth. Appl. Mech. Engng*, **56,** 61–81 (1986).
11. M. S. Rahman and C. H. Hwang, 'A stochatic finite element analysis for the seismic response of earth dams', *Proc. 7th Int. Conf. on Computer Methods and Advances in Geomechanics*, Cairns, Australia, 1991, pp. 857–862.
12. C. H. Yeh, 'Stochastic finite element methods for the seismic reresponse of soils, *Ph.D. Thesis*, Department of Civil Engineering, North Carolina State University, 1995.
13. P. D. Spanos and R. Ghanem, 'Stochastic finite element expansion for random media', *J. Engng. Mech. ASCE*, **115** (5), 1035–1053, (1989).
14. R. Ghanem and P. D. Spanos, 'Polynomial chaos in stochastic finite elements', *J. Appl. Mech, ASME*, **57** (1), 197–202, (1990).
15. H. Jensen and W. D. Iwan, 'Response variability in structural dynamics', *Earthquake Eng. Struct. Dyn.* **20,** 949–959 (1991).
16. H. Jensen and W. D. Iwan, 'Response of systems with uncertain parameters to stochastic excitation', *J. Engng. Mech. ASCE*, **118** (5), (1992).
17. S. Hou, 'Earthquake simulation models and their application', *Ph.D. Thesis*, Department of Civil Engineering, M. I. T., Research Report No. R68-17, 1968.
18. L. Esteva, 'Seismatic risk and seismic design decision', in J. Hansen (ed.), *Seismic Deisng for Nuclear Power Plants*, MIT Press, Cambridge, MA, 1970.

19. E. H. Vanmarcke and P. S. Lai, 'Strong motion duration of earthquakes', *Research Report*, No. R77-16, Department of Civil Engineering, M.I.T. Press, Cambridge, MA, 1977.
20. E. H. Vanmarcke, 'Probabilistic modeling of soil profiles', *J. Geotech. Engng. Div. ASCE.* **103** (GT11)**,** 1227–1246 (1977).
21. E. H. Vanmarcke, *Random Field Analysis and Synthesis*, M.I.T. Press, Cambridge, MA, (1984).
22. I. M. Idriss and H. B. Seed, 'Seismic response of horizontal soil layers', *J. Soil Mech. Found. Engng. ASCE*, **94,** 1003–10031 (1968).
23. S. O. Rice, 'Mathematical analysis of random noise', in N. Wax, (ed.), in: *Bell System Technical Journal*, 1944-23 & 24, pp. 46–156, Reprinted in selected papers in noise and stochastic processes, New York, 1954.
24. M. S. Rahman and C. W. Hwang, A stochastic finite element analysis for the seismic response of soil sites', in: I. Elishankoff and Y. K. Lin (eds.), *Stochastic Structural Dynamics 2*, *New Practical Applications*, 2nd Int. Conf. on Structural Dynamics, Boca Raton, FL 1990, pp. 155–186.
25. H. L. Van Trees, '*Detection*, *Estimation and Modulation Theory*, *Part 1*, Wiley, New York, 1968.
26. C. H. Hwang, 'Stochastic finite element analysis of soils mass under seismic loading', *Ph.D. Thesis*, Department of Civil Engineering, North Carolina State University, 1990.
27. M. Shinozuka, 'Digital simulation of random processes in engineering mechanics with the aid of FTT technique', in: S. T. Ariaratna and H. H. E. Leiphloz (eds.), *Stochastic Problems Mechanics*, University of Waterloo Press, Waterloo, Canada, 1974, pp. 277–286.
28. M. Shinozuka, 'Stochastic fields and their digital simulation', *Lecture Notes for the CISM Course on Stochastic Methods in Structural Mechanics*, Udine, Italy, 1985.
29. M. Shinozuka and C. J. Astill, 'Random eigenvalue problems in structural mechanics', *AIAA. J.* **10** (4)**,** pp. 456–462 (1972).
30. M. Shinozuka and G. Deodatis, 'Response variability of stochastic finite element systems', *Technical Report*, Department of Civil Engineering, Columbia University, New York, 1986.

